Research Square

Preprints are preliminary reports that have not undergone peer review.
They should not be considered conclusive, used to inform clinical practice,
or referenced by the media as validated information.

Hyperoside improves diabetic retinopathy by regulating TGF-β1/miR-200b/VEGF pathway

Xu Yu
Affiliated Hospital of Nanjing University of Chinese Medicine
Hao Wu
Affiliated Hospital of Nanjing University of Chinese Medicine
Lei Zhou
Affiliated Hospital of Nanjing University of Chinese Medicine
Nana Wang
Affiliated Hospital of Nanjing University of Chinese Medicine
Meijie Ben
Affiliated Hospital of Nanjing University of Chinese Medicine
Shasha Li
Nanjing University of Chinese Medicine
Xiaoci Wang
Nanjing University of Chinese Medicine
Jiangyi Yu
Affiliated Hospital of Nanjing University of Chinese Medicine
Yue Zhao (zhaoyuetcm@126.com)
Affiliated Hospital of Nanjing University of Chinese Medicine
Xiqiao Zhou
Affiliated Hospital of Nanjing University of Chinese Medicine

Research Article

Keywords: Hyperoside, retinal endothelial cells, diabetic retinopathy, TGF-β1, miR-200b, VEGF

Posted Date: January 4th, 2023

DOI: https://doi.org/10.21203/rs.3.rs-2376233/v1

License: This work is licensed under a Creative Commons Attribution 4.0 International License.
Read Full License

Abstract

Aims

To evaluate the efficacy of hyperoside and the role of TGF-β1/miR-200b/VEGF pathway in treating diabetic retinopathy (DR).

Methods

(1) Retinal endothelial cells (RECs) were cultured in the normal-glucose group (NG), high-glucose group (HG), mannitol group, high glucose + low-concentration hyperoside group, high glucose + high-concentration hyperoside group, normal glucose + miR-200b inhibitor group (NG + MI), normal glucose + normal control group (NG + NC), high glucose + miR-200b mimic group (HG + MM), and high glucose + normal control group (HG + NC). The viability, migration and tube formation of RECs, and the expressions of TGF-β1, miR-200b and VEGF in each group were detected and compared. (2) Eight Sprague Dawley (SD) rats were used in the normal control group, and 32 SD rats established DR models were randomly divided into the four groups for DR group (DR), DR + low-dose hyperoside group, DR + high-dose hyperoside group, and DR + Calcium Dobesilate group. The tissue pathology and vasculopathy of rat retina, and the expressions of TGF-β1, miR-200b, and VEGF of retinal tissues in different group were tested and compared.

Results

(1) Excessive proliferation, migration and tube formation of RECs were induced by high glucose. The expressions of TGF-β1 and VEGF in HG were markedly up-regulated, but miR-200b levels were obviously down-regulated. However, hyperoside could significantly reverse the expressions of TGF-β1, VEGF and miR-200b; and inhibit high-glucose-induced over-proliferation of RECs dose-dependently. RECs viability and VEGF level were much higher in NG + MI than for NG but lower in HG + MM than for HG, while miR-200b level was substantially lower in NG + MI than for NG but higher in HG + MM than for HG. (2) The retinal pathological changes and vasculopathy in DR rats were more serious compared with normal rats. TGF-β1 and VEGF levels in DR rats retina were markedly up-regulated, while miR-200b levels were obviously down-regulated. However, hyperoside could notably reverse the expressions of TGF-β1, VEGF, and miR-200b in DR rat retina and alleviate retinal tissue injury and vascular lesions of DR rats dose-dependently.

Conclusion

Hyperoside could treat DR by regulating TGF-β1/miR-200b/VEGF pathway.

Background

Diabetic retinopathy (DR) is one of major microvascular complications of diabetes mellitus (DM) and the leading cause of vision loss in middle-aged and elderly people around the world (1). A global meta-analysis including 35 studies has showed that the incidence of DR in DM was approximately 34.6%, specifically including 6.96% proliferative diabetic retinopathy, 6.81% diabetic macular edema, and 10.2% vision-threatening diabetic retinopathy (2). With the growing prevalence and prolonged duration (3), DR has been increasingly harmful to human health and burdened the medical care system. Therefore, it is outstandingly positive to explore effective treatment and corresponding mechanism for preventing the progression of DR.

According to Diabetic Retinopathy Preferred Practice Pattern Guideline (Version 2019) issued by American Academy of Ophthalmology (4), healthy lifestyle and strict control of blood glucose, blood pressure and serum lipid are beneficial to DR prevention. However, the progression of diabetic complication seems more than hard to repress. The validity of many anti-DR drugs such as alprostadil, antioxidants, antithrombotics, and protein kinase-C inhibitors needs further evaluations from large-sample, multi-center clinical researches (5). To solve this dilemma, some complementary and alternative treatments via traditional herbal medicine were tentatively used for DR. Interestingly, more and more herbal medicines showed a potential and promising efficacy against DR (6).

The recent clinical study of our team indicated that *Abelmoschus manihot* could improve the severity of DR, ETDRS vision scores and macular edema in type 2 diabetes, and the specific therapeutic mechanism seemed to be associated with inhibited vascular endothelial growth factor (VEGF) levels, which needed further investigations (7). Previous studies have showed that the activation of transforming growth factor-beta 1 (TGF-β1)/micro-RNA 200b (miR-200b)/VEGF pathway by high glucose might play an essential role in the destruction of blood-retinal barrier (BRB) and the pathogenesis of DR (8–10). Meanwhile, the related studies have also shown that hyperoside, as the main active ingredient of *Abelmoschus manihot* (11), could inhibit the expression of TGF-β1 in glomerular mesangial cells under high glucose condition (12). It would need the further study of whether hyperoside also played a role in treating DR by improving TGF-β1/miR-200b/VEGF pathway. Therefore, the present study was primarily concerned with the hyperoside's effects on DR pathological process including the retinal injury of diabetic rats, the proliferation of retinal endothelial cells (RECs), and the regulation of TGF-β1/miR-200b/VEGF pathway in high glucose. Moreover, it was hoped to explore the preliminary effect and mechanism of hyperoside in the treatment of DR.

Materials And Methods

2.1 Hyperoside

Hyperoside extracted from *Abelmoschus manihot* was purchased from the agent company (Meilunbio/O0807AS). The characteristics of the hyperoside are as follows: (1) Chemical Abstracts

Service number: 482-36-0; (2) Appearance: Yellow crystalline powder is stored in cool, dry, airproof and innocuous condition with limited light and heat; (3) Purity: The purity assayed by high performance liquid chromatography is 99.45%.

2.2 Cell culture and treatments

A vial for primary human RECs was purchased from the cell company (Cell Systems/ACBRI-181). RECs were cultured in complete growth medium which consisted with 89% low-glucose Dulbecco's Modified Eagle Medium (DMEM, GIBCO/11885092), 10% fetal bovine serum (FBS, GIBCO/10099141), and 1% antibiotics (100U/mL penicillin and 100ug/mL streptomycin) at 37 ℃ in a humidified atmosphere of 5% CO2. When the flask existed approximately 90% confluence, RECs could be subcultured. The cell-culturing experiments included three parts: (1) The subcultured RECs were randomly divided into five groups with different glucose concentrations in the culture mediums: normal-glucose group (NG, 5 mmol/L glucose), high-glucose group 1 (HG-1, 20 mmol/L glucose), high-glucose group 2 (HG-2, 25 mmol/L glucose), high-glucose group 3 (HG-3, 30 mmol/L glucose), and high-glucose group 4 (HG-4, 35 mmol/L glucose); (2) The subcultured RECs were also randomly assigned into the five other groups for normal-glucose group (NG, 5 mmol/L glucose), high-glucose group (HG, 35 mmol/L glucose), mannitol group (MG, 5 mmol/L glucose plus 30 mmol/L mannitol as an osmotic pressure control), high glucose + 100 ug/ml hyperoside group (HG + H100), high glucose + 400 ug/ml hyperoside group (HG + H400). The hyperoside was dissolved in 0.1% dimethyl sulfoxide solution for RECs treatment; (3) The subcultured RECs were randomly divided into another six groups: normal-glucose group (NG, 5 mmol/L glucose), normal glucose + miR-200b inhibitor group (NG + MI, normal glucose plus miR-200b inhibitor and transfection reagent), normal glucose + normal control group (NG + NC, normal glucose plus only transfection reagent), high-glucose group (HG, 35 mmol/L glucose), high glucose + miR-200b mimic group (HG + MM, high glucose plus miR-200b mimic and transfection reagent), and high glucose + normal control group (HG + NC, high glucose plus only transfection reagent).

2.3 Cell counting kit-8 (CCK-8) assay

The RECs were plated in 96-well plates with 6×10^3 cells per well. The cells were serum-starved for 24 hours after adherence, followed by different managements including various concentrations glucose and hyperoside treatments as described above. Subsequently, RECs were incubated with 10 μL CCK-8 agent (Dojindo/CK04) for 3 hours. The optical density at 450 nm of each well was determined by a microplate reader (PerkinElmer EnSpire) to calculate the relative viability of RECs.

2.4 Transwell assay

The RECs (2×10^4 cells per well) and various concentrations glucose and hyperoside mediums were respectively added to the upper chamber of 24-well transwell inserts (8 μm pore size, Labselect/14341).

As for the lower chamber, the medium containing 20% FBS and 5 mmol/L glucose was added, and the follow-up culture was performed at 37°C for 24 h. The RECs at the bottom of the upper chamber were stained with 0.5% crystal violet and the cells inside the upper chamber were removed with a cotton swab. The RECs outside the bottom of upper chamber were observed and counted under a light microscope (Olympus/CKX31) at 200× magnification in five random visual fields.

2.5 Cell tube formation assay

The Matrigel matrix glue (10mg/mL, Corning/356234) was slowly injected into a 96-well plate placed in an ice bath with a pre-cooled pipette. The volume of injection in each well was 100 μL. The Matrigel matrix glue was then placed in an incubator at 37°C for 30 min to solidify the glue. Then, the cultured cells were inoculated into the 96-well plate with 1×10^4 cells per well. Meanwhile, the different mediums as described above were respectively added into the plate and then continuously cultured for another 6 hours. The tubular structure was recorded by a light microscope (Olympus/CKX31) and the branch points were visualized and calculated in five random regions.

2.6 Cell transfection

The miR-200b mimic and inhibitor were purchased from GenePharma company and transfected into RECs according to the manufacturer's instructions. Firstly, cells were seeded in complete medium for 24 hours to grow to 30% confluence before transfection. Then the DMEM without serum was used to dilute the miR-200b mimic/inhibitor and the transfection reagent (Engreen/R4000). Subsequently, these two diluents were mixed and kept stable for 15 minutes. The mixed liquid was added to RECs with complete medium. After 24 hours of incubation in a 5% CO_2 humidified atmosphere at 37℃, the transfection medium could be replaced with NG or HG complete mediums for another 24 hours before subsequent experiments.

2.7 Animals

Forty specific pathogen-free healthy male Sprague Dawley (SD) rats (five to six weeks old) weighing from 170–200 g were purchased from Qing Long Shan Animal Centre (Nanjing, China). These rats were treated and operated according to the guidelines of Animal Ethics Committee of Affiliated Hospital of Nanjing University of Chinese Medicine (Ethic approve number: 2020DW-21-02). Rats were housed at constant room temperature (20–22℃) and relative humidity (50–60%) under a controlled 12-hour light/dark cycle and had free access to water and the standard laboratory diet.

2.8 DR rats model and drug treatment

Eight SD rats were randomly selected as normal control group (NC), and the other 32 rats were used to establish DR models which were randomly divided into the four groups including DR group (DR models with no treatment), DR + low-dose hyperoside group (DR + L-HY, DR models with 6.5 mg hyperoside per 1 kg rat body mass per day, 6.5 mg/kg/d), DR + high-dose hyperoside group (DR + H-HY, DR models with 19.5 mg/kg/d hyperoside), and DR + Calcium Dobesilate group (DR + CD, DR models with 135 mg/kg/d Calcium Dobesilate). DR models were established as follows: (1) After 4 weeks of high-fat diet (rodent diet with 45% calories from fat), SD rats were fasted for 12 hours, and then intraperitoneally injected with 1% streptozotocin (STZ, Sigma-Aldrich/V900890) solution at the dose of 25 mg/kg, and injected again at the same dose after 2 days. The random blood glucose of every SD rat was measured at 72 hours after injection and all blood glucose levels were > 16.7 mmol/L, then DM models were considered successful. (2) DM rats were allowed to eat and drink normally, their blood glucose and body mass (BM) were measured regularly, and morphological changes were observed throughout the study. After the 8-week continuous feeding, one NC and two DM rats were randomly selected and their retinal tissue pathology and trypsin digest were examined to evaluate the successful DR models. After DR models had been established, groups of DR + L-HY, DR + H-HY and DR + CD were given respective doses of hyperoside and Calcium Dobesilate which were dissolved in 0.5% sodium carboxymethyl cellulose solution by gavage. Meanwhile, groups of NC and DR were given equal amount of 0.5% sodium carboxymethyl cellulose solution. All rats were continuously given food, water, and drugs for 8 weeks and then anesthetized to death. The eyeballs were isolated and made into optic cups for further experiments.

2.9 Retinal pathology

The retinal tissues were carefully isolated after optic cups were fixed with 4% paraformaldehyde for 24 hours. The tissues were then dehydrated in a concentration gradient of alcohol, made transparent with xylene, and followed by paraffin embedding. The paraffin-embedded tissue blocks were cut into 4-μm thick sections. After xylene dewaxing and gradient alcohol rehydration, the tissue sections were stained with hematoxylin-eosin (HE) staining solution (biosharp/BL-700A). The pathological changes of retinal tissues in all groups were observed under a light microscope (Olympus/CKX31) after the tissue sections were dehydrated by gradient alcohol, made transparent via xylene, and sealed with neutral resin.

2.10 Retinal trypsin digest

To analyze the vasculopathy for retinal capillary degeneration, RECs proliferation, and retinal pericytes (RPCs) loss, we used the retinal trypsin digest technique as follows: The retinal tissues were isolated and digested in 3% trypsin solution (GIBCO/25200-072) at 37℃ for 2 hours; the dissolved retina was moved into distilled water with a glass rod and gently shaken to wash away the inner boundary membrane and residual retinal nerve tissue; and then the retinal vascular network, which had been fully digested and separated, was lifted with the glass rod and quickly transferred to a glass slide for full spreading and natural drying. The slides were stained with periodic acid-schiff (PAS, solarbio/G1285) and observed

under a microscope (Olympus/CKX31). The retinal vascular quantity (RVQ) and endothelial cells to pericytes ratio (E/P) in all groups were counted and compared under the microscope. RVQ calculation method was as follows: at 200× magnification, five regions of each rat's retinal vascular network were randomly selected, and the numbers of capillaries passing through the transverse diameter and vertical diameter of the center of each region were calculated and averaged; the mean number of five regions was taken as the RVQ of this sample. E/P calculation method was similar to RVQ: at 400× magnification, five visual fields of each rat's retinal vascular network were randomly selected; the number and ratio of RECs and pericytes in each visual field were calculated, and the mean value of five visual fields was used as the E/P value of the rat.

2.11 Retinal immunofluorescence (IF) detection

The retinal tissue sections were incubated with 3% H_2O_2 at room temperature for 10 minutes, followed by antigen repair for 15 minutes and goat serum sealing for 20 minutes. Then the sections were incubated with TGF-β1 primary antibody (Sigma/SAB4502954) at 4℃ for 12 hours, followed by incubation with secondary antibody with FITC (AAT Bioquest/16868) at 37℃ in darkness for 30 minutes. After washing with PBS, each section was added with DAPI (Sigma-Aldrich/D9542) and incubated at 37℃ in darkness for 5 minutes. Finally, the expression of TGF-β1 protein in retinal tissue section was observed under a fluorescence microscope (Olympus/BX43). The expression of VEGF protein in retinal tissue was detected with specific antibodies through the similar process.

2.12 Western blotting (WB) assay

After measuring the concentrations of total proteins from retinal tissues or RECs lysates by BCA protein assay kit (Abcam/ab102536), the proteins were separated by SDS-PAGE and then transferred to PVDF membranes (BIO-RAD/1620177). Next, the membranes were blocked with 5% skim milk for 1 hour, followed by incubation with TGF-β1 rabbit antibody (Cell Signaling Technology/3709S) for 14 hours at 4℃ and goat anti-rabbit IgG-HRP (Sigma/A0545) for 1 hour at 37℃. The immune complex was detected using the enhanced chemiluminescence by ECL kit (Merck millipore/wbklso500). After exposure and development, the gray value of each band was quantified, and the relative levels of TGF-β1 protein to β-actin were determined by the imaging system (ImageQuant LAS 4000). The VEGF protein expressions were detected with corresponding primary and secondary antibodies by the above-mentioned methods.

2.13 Quantitative real-time reverse transcription polymerase chain reaction (qRT-PCR) analysis

Total RNA was extracted from retinal tissues or RECs by RNA extraction kit (ThermoFisher/15596018) and subjected to reverse transcription via reverse transcription kit (Invitrogen/4368814). Samples were amplified by DNA polymerase (Roche/11146173001) using specific primers by qRT-PCR system (Applied Biosystems 7500). The relative expression levels of miRNAs (miR-200b) and mRNAs (TGF-β1 and VEGF) normalized by U6 small nuclear RNA and β-actin mRNA, respectively, were calculated by $2^{-\Delta\Delta Ct}$ method.

2.14 Statistical analysis

All experiments were repeated three times. Results were expressed as mean ± standard deviation. The difference among groups was statistically analyzed by one-way ANOVA using GraphPad Prism 8 software. $P < 0.05$ was considered significantly different.

Results

3.1 High glucose induced excessive proliferation of RECs

To evaluate the effect of high glucose on the proliferation of RECs, the RECs were cultured with different concentrations of high glucose, and the viability of RECs were measured at varied incubation times, which were compared with normal-glucose group. As shown in Fig. 1A, the RECs viability in HG-1 was significantly elevated compared with NG at the 24-hour period (1.12 ± 0.04 vs. 1.00 ± 0.00, $P < 0.01$). Meanwhile, the RECs viability in HG-2 was also greatly elevated compared with NG at the 24-hour, 48-hour and 72-hour period, respectively (1.21 ± 0.04 vs. 1.00 ± 0.00, $P < 0.01$; 1.11 ± 0.02 vs. 1.00 ± 0.00, $P < 0.01$; 1.08 ± 0.03 vs. 1.00 ± 0.00, $P < 0.01$). For other comparisons, such as HG-3 vs. NG and HG-4 vs. NG at the 24-hour, 48-hour, 72-hour period, respectively, all the findings suggested that the viability of RECs had a more significant relation with the increase of high glucose concentration. These results indicated that high glucose could induce excessive proliferation of RECs.

3.2 Hyperoside inhibited excessive proliferation of RECs in high glucose

We evaluated the effects of hyperoside against high-glucose-induced excessive viability of RECs. Excessive proliferation of RECs is an early process of BRB destruction and DR occurrence. Inhibition of hyperoside on over-proliferation of RECs under high glucose condition would significantly improve DR. As presented in Fig. 1B, all RECs viability levels in HG at different incubation periods (24, 48, and 72 h) were higher than for NG groups (1.11 ± 0.04 vs. 1.00 ± 0.00, $P < 0.05$; 1.26 ± 0.07 vs. 1.00 ± 0.00, $P < 0.01$; 1.10 ± 0.03 vs. 1.00 ± 0.00, $P < 0.05$). Meanwhile, all RECs viability levels in HG + H100 at different treatment periods were lower than HG groups (1.03 ± 0.02 vs. 1.11 ± 0.04, $P < 0.05$; 1.05 ± 0.11 vs. 1.26 ± 0.07, $P < 0.01$; 0.94 ± 0.04 vs. 1.10 ± 0.03, $P < 0.01$). The similar difference was also seen in comparisons of HG + H400 vs. HG and HG + H400 vs. HG + H100. The results showed that both low-concentration (100 ug/mL) and high-concentration (400 ug/mL) hyperoside could significantly inhibit RECs viability under high glucose condition, and the stronger inhibition of RECs viability was along with the increase of hyperoside concentration. These data suggested that hyperoside could dose-dependently inhibit excessive proliferation of RECs in high glucose.

3.3 Hyperoside inhibited excessive migration and tube formation of RECs in high glucose

It is well known that DR may include not only RECs proliferation, but also significantly increased migration and tube formation of RECs. Therefore, we measured the role of hyperoside for the migration and tube formation of RECs in high glucose. As shown in Fig. 2A,C, the number of migrated RECs in HG was significantly higher than that in NG (375.7 ± 10.4 vs. 133.3 ± 9.6, $P < 0.01$), and also higher than HG + H100 and HG + H400 (375.7 ± 10.4 vs. 234.7 ± 6.5, $P < 0.01$; 375.7 ± 10.4 vs. 137.0 ± 9.0, $P < 0.01$). Similar results were also seen in the tube formation assay as presented in Fig. 2B,D, the number of branch points of RECs in HG was significantly higher than that in NG (38.0 ± 4.0 vs. 9.3 ± 1.5, $P < 0.01$), meanwhile, the numbers in HG + H100 and HG + H400 were significantly decreased compared with HG (21.0 ± 3.6 vs. 38.0 ± 4.0, $P < 0.01$; 10.3 ± 1.5 vs. 38.0 ± 4.0, $P < 0.01$). These data suggested that hyperoside could inhibit excessive migration and tube formation of RECs induced by high glucose.

3.4 TGF-β1/miR-200b/VEGF pathway contributed to over-proliferation of RECs in high glucose

To estimate the role of TGF-β1/miR-200b/VEGF pathway in the over-proliferation of RECs induced by high glucose, we, respectively, transfected miR-200b mimic and miR-200b inhibitor into RECs in high-glucose and normal-glucose condition. As shown in Fig. 3, miR-200b inhibitor in NG + MI could significantly elevate RECs viability (1.20 ± 0.15 vs. 1.00 ± 0.00, $P < 0.05$, Fig. 3A) and expressions of VEGF mRNA and protein (1.76 ± 0.27 vs. 1.00 ± 0.00, $P < 0.05$; 2.96 ± 0.39 vs. 1.00 ± 0.00, $P < 0.01$, Figs. 3B,C), but reduce VEGF miR-200b expression (0.57 ± 0.12 vs. 1.00 ± 0.00, $P < 0.05$, Fig. 3B) compared with NG. However, miR-200b mimic in HG + MM could significantly down-regulate RECs viability (0.95 ± 0.15 vs. 1.22 ± 0.10, $P < 0.01$, Fig. 3A) and VEGF mRNA and protein levels (0.94 ± 0.16 vs. 2.19 ± 0.58, $P < 0.01$; 1.59 ± 0.13 vs. 3.70 ± 0.35, $P < 0.01$, Figs. 3B,C), but up-regulate VEGF miR-200b expression (4.91 ± 1.00 vs. 0.45 ± 0.18, $P < 0.01$, Fig. 3B) compared with HG. There were no significant differences of TGF-β1 mRNA and protein expressions between NG and NG + MI. Also, there were no significant differences of TGF-β1 mRNA and protein expressions between HG and HG + MM. The expressions of TGF-β1 mRNA and protein were notably enhanced by high glucose but not regulated by miR-200b mimic or inhibitor (Figs. 3B,C). These results indicated that the high-glucose-induced activation of TGF-β1/miR-200b/VEGF pathway played a positive role in excessive proliferation of RECs.

3.5 Hyperoside regulated TGF-β1/miR-200b/VEGF pathway in high-glucose-cultured RECs

To elucidate the protective mechanism of hyperoside against RECs over-proliferation in HG, we analyzed the variation of TGF-β1, miR-200b, and VEGF levels in different groups. Compared with NG, HG could remarkably induce high mRNAs and proteins expressions of TGF-β1 and VEGF (3.08 ± 0.35 vs. 1.00 ± 0.00, $P < 0.01$; 1.80 ± 0.09 vs. 1.00 ± 0.00, $P < 0.01$ & 4.82 ± 1.08 vs. 1.00 ± 0.00, $P < 0.01$; 2.25 ± 0.16 vs. 1.00 ± 0.00, $P < 0.01$, Figs. 4A,B), and obviously inhibit miR-200b expressions (0.39 ± 0.13 vs. 1.00 ± 0.00, $P < 0.05$, Fig. 4A). However, hyperoside reversed the expressions of TGF-β1/miR-200b/VEGF under high

glucose condition. As presented in Fig. 4, the low concentration of hyperoside in HG + H100 could significantly inhibit mRNA and protein levels of TGF-β1 and VEGF (1.54 ± 0.14 vs. 3.08 ± 0.35, $P < 0.01$; 1.39 ± 0.08 vs. 1.80 ± 0.09, $P < 0.01$ & 2.82 ± 0.43 vs. 4.82 ± 1.08, $P < 0.01$; 1.92 ± 0.09 vs. 2.25 ± 0.16, $P < 0.05$, Figs. 4A,B), and up-regulate miR-200b levels (1.06 ± 0.10 vs. 0.39 ± 0.13, $P < 0.05$, Fig. 4A) compared with HG. The similar difference was also seen in comparisons of HG + H400 vs. HG and HG + H400 vs. HG + H100. There was a stronger regulation of TGF-β1/miR-200b/VEGF pathway when hyperoside concentration increased. Therefore, these data indicated that hyperoside could decrease TGF-β1 and VEGF, but increase miR-200b of RECs under high glucose condition in a dose-dependent manner.

3.6 Body mass and fasting blood glucose of rats in different groups

We observed BM and fasting blood glucose (FBG) of rats at different periods including at 4 weeks before STZ injection (-4 w), 0 week before STZ injection (0 w), 8 weeks after STZ injection (8 w), and 16 weeks after STZ injection (16 w). As shown in Fig. 5, there were no significant differences of BM and FBG at -4 w in all groups. After 4 weeks of high-fat diet, BM and FBG results in all DR groups (DR, DR + L-HY, DR + H-HY & DR + CD) were significantly higher than NC. At 8 w and 16 w, BM results in all DR groups were significantly lower than NC, while FBG results were significantly higher than NC. However, there were no significant difference of BM and FBG in DR, DR + L-HY, DR + H-HY or DR + CD groups at any time. It could be speculated that the primary effect of hyperoside and Calcium Dobesilate was not aimed at hyperglycemia.

3.7 Hyperoside improved pathology of retinal tissue

To further analyze the possible role of hyperoside on retinal injury in diabetic rats, we observed the pathological changes of retinal tissues in NC, DR, DR + L-HY, DR + H-HY and DR + CD groups. As shown in Fig. 6A, in NC group, the ganglion cell layer (GCL) in retinal tissue was orderly, and the inner nuclear layer (INL) and outer nuclear layer (ONL) were closely arranged. In DR group, the arrangement of GCL was disordered, and INL and ONL appeared sparser and less compact than NC. However, these pathological changes were alleviated in DR + L-HY group, and improved in DR + H-HY and DR + CD groups as marked by black arrows in Fig. 6A. These results indicated that hyperoside could alleviate retinal tissue damage in DR rats.

3.8 Hyperoside improved retinal vasculopathy

To confirm the improvement of hyperoside on diabetic retinal injury, we also evaluated the effect of hyperoside on retinal vessels in DR rats. Retinal trypsin digest and retinal vascular staining were performed in NC, DR, DR + L-HY, DR + H-HY and DR + CD groups. In NC group, the retinal capillaries distributed regularly with smooth vascular branches, uniform diameter and very few acellular capillaries.

In DR group, the retinal capillary network remained dense, disorderly and twisted, with uneven diameter, more acellular capillaries (AC), more ghost-pericytes (GP), and proliferative RECs. However, these retinal vasculopathy were alleviated in DR + L-HY group, and improved in DR + H-HY and DR + CD groups as shown in Fig. 6B. These preliminary results showed the improvement of hyperoside on diabetic retinal vasculopathy.

3.9 Comparisons of RVQ and E/P to evaluate the degrees of retinal vasculopathy

As mentioned above, RVQ and E/P were further calculated to quantitatively assess the alleviation of hyperoside in diabetic retinal vascular lesions. As shown in Table 1, RVQ and E/P in DR groups were significantly higher than NC (30.33 ± 3.83 vs. 14.83 ± 2.04, $P < 0.01$; 2.43 ± 0.22 vs. 1.03 ± 0.12, $P < 0.01$), but all RVQ and E/P in DR + L-HY, DR + H-HY and DR + CD groups were significantly lower than DR. In addition, RVQ and E/P in DR + H-HY were significantly lower than DR + L-HY (19.83 ± 2.32 vs. 24.50 ± 2.88, $P < 0.05$; 1.52 ± 0.18 vs. 1.83 ± 0.13, $P < 0.05$). These results indicated that hyperoside could alleviate retinal vasculopathy severity of DR rats, and the alleviation effect was more strengthened with the increase of hyperoside dose.

Table 1
Comparisons of RVQ and E/P of retinal capillaries in different groups

	NC (n = 6)	DR (n = 6)	DR + L-HY (n = 6)	DR + H-HY (n = 6)	DR + CD (n = 7)
RVQ	14.83 ± 2.04	30.33 ± 3.83**	24.50 ± 2.88$^{\#\#}$	19.83 ± 2.32$^{\#\#\Delta}$	19.86 ± 1.57$^{\#\#}$
E/P	1.03 ± 0.12	2.43 ± 0.22**	1.83 ± 0.13$^{\#\#}$	1.52 ± 0.18$^{\#\#\Delta}$	1.27 ± 0.07$^{\#\#}$

RVQ: retinal vascular quantity; E/P: endothelial cells to pericytes ratio. Data are presented as mean ± standard deviation. $P < 0.05$ is statistically significant. ** vs. NC, $P < 0.01$; $^{\#\#}$ vs. DR, $P < 0.01$; $^{\Delta}$ vs. DR + L-HY, $P < 0.05$.

3.10 Hyperoside regulated TGF-β1/miR-200b/VEGF pathway in retinal tissues of DR rats

Finally, we compared the expressions of TGF-β1, miR-200b and VEGF in retinal tissues of all groups by qRT-PCR, WB and IF. The mRNAs and proteins expressions of TGF-β1 and VEGF in DR were significantly higher than NC (4.25 ± 0.72 vs. 1.00 ± 0.00, $P < 0.01$; 3.41 ± 0.39 vs. 1.00 ± 0.00, $P < 0.01$ & 3.97 ± 0.51 vs. 1.00 ± 0.00, $P < 0.01$; 4.93 ± 0.53 vs. 1.00 ± 0.00, $P < 0.01$, Figs. 7A,B), while the miR-200b in DR was significantly lower than NC (0.19 ± 0.07 vs. 1.00 ± 0.00, $P < 0.01$, Fig. 7A). However, hyperoside reversed the expressions of TGF-β1/miR-200b/VEGF in DR group. As shown in Fig. 7A,B, the low-dose hyperoside (in DR + L-HY), high-dose hyperoside (in DR + H-HY), and Calcium Dobesilate (in DR + CD) all significantly

inhibited mRNAs and protein levels of TGF-β1 and VEGF, and up-regulated miR-200b levels compared with DR groups (0.48 ± 0.10 vs. 0.19 ± 0.07, P < 0.05; 0.77 ± 0.14 vs. 0.19 ± 0.07, P < 0.01; 1.09 ± 0.08 vs. 0.19 ± 0.07, P < 0.01, Fig. 7A). The comparison between DR + L-HY and DR + H-HY further showed that the stronger regulations of TGF-β1, VEGF, and miR-200b were along with the increase of hyperoside dose. Meanwhile, the similar differences of TGF-β1 and VEGF in all groups were also shown in Fig. 7C. In DR group, the green fluorescence intensities representing TGF-β1 and VEGF expression levels were significantly stronger than for NC group. However, the green fluorescence intensity of DR + L-HY group was significantly weaker than for DR group. In DR + H-HYand DR + CD group, the green fluorescence intensities were further weakened. Therefore, these data suggested that hyperoside could down-regulate TGF-β1 and VEGF, but up-regulate miR-200b in retinal tissues of DR rats.

Discussion

TGF-β is a protein family which has multifunctional and bidirectional intercellular signaling. Different isoforms (e.g. TGF-β1, TGF-β2, and TGF-β3) are highly homologous in structure, and their functions are quite similar. TGF-βs are synthesized and secreted as precursor proteins, which are combined with latency-associated peptide in an inactivated manner. After latency-associated peptide is cleaved, TGF-βs are activated and can bind to specific receptors on cell surface and play essential roles in growth and development, inflammation and repair and host immunity (13, 14). The recent studies showed that TGF-β1 was up-regulated by high glucose and considered a proinflammatory cytokine that could be implicated in the pathogenesis of DR (15). Elevated TGF-β1 specifically bounded to its receptor on cell surface and transmitted the signal to intracellular Smads proteins (16), which continued to transmit the signal into the nucleus to inhibit the activity of miR-200b promoter and reduce the expression of miR-200b (17, 18). The miR-200b was an endogenous non-coding RNA that did not participate in protein coding, but precisely bound to the 3' non-coding region of VEGF mRNA to inhibit VEGF mRNA translation and protein synthesis (19, 20). The previous studies have proven that over-expression of VEGF played an essential role in RECs dysfunction induced by high glucose (21) and contributed to BRB destruction in several blinding eye diseases including DR (22, 23). However, the detailed mechanisms have been not illustrated clearly. Therefore, the evaluation of TGF-β1/miR-200b/VEGF pathway in DR pathogenesis is the first aim of our study.

We used CCK-8 assay to evaluate the proliferation of RECs. There are many methods to detect cell proliferation, among which EdU reflects cell proliferation by detecting the replication activity of DNA, PCNA and Ki67 reflect cell proliferation by detecting the level of nuclear antigen of cells in the proliferation stage, while CCK-8 indirectly reflects the number of living cells by detecting the metabolic activity of cells. Admittedly, EdU, PCNA and Ki67 reflect cell proliferation more directly. However, CCK-8 has its own advantages, such as simple operation, high sensitivity, accurate results, good repeatability, low cytotoxicity, no radioactivity and so on. Both DNA-related tests (EdU, PCNA & Ki67) and metabolism-related test (CCK-8) supported the same conclusion uniformly. In this study, the CCK-8 was used to confirm that excessive proliferation of RECs were induced by high glucose, which has been applied in many previous studies (24, 25). The focus of this study was to confirm the proliferation of RECs induced

by high glucose and inhibited by hyperoside. In addition, we further assayed migration and tube formation of RECs to evaluate the role of high-glucose and hyperoside on RECs dysfunction. All results including CCK-8, transwell and tube formation of RECs should be sufficient to draw the conclusion.

The results of our experiments *in vitro* showed that the proliferation, migration and tube formation of RECs were more significantly related with the increase of glucose concentration, while this promoting effect was not seen in the same concentration of mannitol. These results suggested that over-proliferation of RECs and retinal angiogenesis was mainly driven by high glucose rather than high osmotic pressure (26). Meanwhile, high glucose remarkably induced an increase in expressions of TGF-β1 and VEGF, and decreased expression of miR-200b in RECs, which was similar to the results in previous studies (27). However, after miR-200b mimic was transfected into RECs under high glucose condition, TGF-β1 level was also significantly elevated. The RECs viability and the expression of VEGF were obviously decreased, while the expression of miR-200b was significantly increased. In contrast, after miR-200b inhibitor was transfected into RECs under normal glucose condition, the RECs viability and the expression of VEGF were significantly enhanced, while the expression of miR-200b was significantly reduced. The above transfection experiments suggested that the activation of TGF-β1/miR-200b/VEGF pathway played a pivotal role in RECs proliferation and retinal angiogenesis induced by high glucose. There are many mechanisms resulting in DR, including inflammation, pyroptosis, retinal neovascularization, epigenetic modification, perturbation of the redox system, and the interference of mi-RNA (28). The TGF-β1/miR-200b/VEGF pathway may not be the only mechanism, but it must be a crucial mechanism of DR pathogenesis.

Our previous study has proven that *Abelmoschus manihot* could improve DR severity, ETDRS vision, macular edema, and serum VEGF levels in type 2 diabetes (7). Hyperoside is a primary active ingredient of *Abelmoschus manihot* (29), and the hyperoside content level in *Abelmoschus manihot* is notably higher compared with other herbal medicines (30). Hyperoside is also one of the flavonoid glycosides with anti-inflammatory, antioxidant, antidepressant, and anti-cancer effects (31, 32). Recent studies have confirmed that hyperoside could improve oxidative stress and inflammation induced by high glucose (33, 34), and inhibit the over-expression of TGF-β1 under high-glucose condition (35). Can this explain the therapeutic mechanism of *Abelmoschus manihot* against DR? What is the role of TGF-β1/miR-200b/VEGF pathway in the treatment of DR by hyperoside? These issues need more illustrations.

Our further *in vitro* experiments have shown that both low-concentration and high-concentration hyperoside could inhibit proliferation, migration and tube formation of RECs induced by high glucose, and the inhibition was obviously strengthened with the elevation of hyperoside concentration. Meanwhile, hyperoside also significantly down-regulated the activation of TGF-β1/miR-200b/VEGF pathway in RECs proliferation induced by high glucose, and the regulation was obviously enhanced with the increase of hyperoside concentration. In addition, the results of *in vivo* experiments showed that retinal ganglion cell layers of DR group were disordered, and the inner and outer nuclear layers were sparsely arranged. It was suggested that the retinal damage of DR group was relatively severe, and the lesion had broken through BRB and spread to optic nerve cells. Furthermore, it was convincing that E/P and RVQ were used as

representative indicators to assess the degrees of retinal capillary degeneration and neovascularization in DR (36, 37). The results showed that E/P and RVQ in DR group were significantly higher than NC group, and RECs proliferation and angiogenesis also increased obviously in DR group. In contrast, hyperoside could significantly improve retinal tissue injury and vascular lesions in DR group, and the efficacy was amplified with the elevation of hyperoside dose. These results preliminarily confirmed that hyperoside could treat DR.

The related WB, IF and PCR results showed that hyperoside also conspicuously decreased the expressions of TGF-β1 and VEGF in retinal tissues of DR rats, but markedly increased the expression of miR-200b. These results further confirmed the inhibitory effect of hyperoside on TGF-β1/miR-200b/VEGF pathway. Interestingly, the comparisons of FBG levels of DR rats in all groups at 0 w, 8 w, and 16 w showed that all FBG levels in DR group, DR + L-HY group, DR + H-HY group, and DR + CD group were higher than that for NC group, but there was no significant difference of FBG levels in all DR rats groups. These data suggested that the therapeutic effect of hyperoside on DR rats was not dependent on the decrease of blood glucose, which was different from previous reports that some herbal medicines could improve diabetic complication by hypoglycemic method (38, 39). However, it is known that the "metabolic memory" effect caused by long-term hyperglycemia can lead to an embarrassing situation that many DM patients cannot prevent the progression of diabetic complications despite significant improvement of blood glucose (40, 41). Therefore, it is particularly important to explore effective methods to improve DR independent of glycemic control. The results of this study showed that hyperoside treated DR by inhibiting TGF-β1/miR-200b/VEGF pathway rather than lowering blood glucose. Hyperoside can be regarded as a potential effective complementary and alternative treatment for DR.

Due to time and funds limitation, it is a pity that some experiments are not performed, such as the evaluation of RECs proliferation by EdU or Ki67, and the possible inhibitory mechanism of RPCs loss by hyperoside and so on. RPCs loss is regarded as an essential pathogenic process in BRB dysfunction (42) and the completion of related experiments will be more evidential for full explanation of DR pathogenesis. These deficiencies will be improved in further similar studies.

Conclusions

In summary, the present study offered convincing evidence that hyperoside can improve RECs over-proliferation and angiogenesis induced by high-glucose and alleviate retinal tissue injury and vascular lesions in DR rats. The therapeutic mechanism is probably attributed to the regulation of TGF-β1/miR-200b/VEGF pathway by hyperoside. These results can be taken as a novel exploration of treatment strategy for DR.

Abbreviations

acellular capillaries (AC), blood-retinal barrier (BRB), body mass (BM), Calcium Dobesilate (CD), diabetes mellitus (DM), diabetic retinopathy (DR), endothelial cells to pericytes ratio (E/P), fasting blood glucose

(FBG), ganglion cell layer (GCL), ghost-pericytes (GP), hyperoside (HY), inner nuclear layer (INL), micro-RNA 200b (miR-200b), outer nuclear layer (ONL), retinal endothelial cells (RECs), retinal pericytes (RPCs), retinal vascular quantity (RVQ), streptozotocin (STZ), transforming growth factor-beta 1 (TGF-β1), vascular endothelial growth factor (VEGF)

Declarations

Ethics approval and consent to participate

The SD rats used in this research were treated and operated according to the guidelines of Animal Ethics Committee of Affiliated Hospital of Nanjing University of Chinese Medicine (Ethic approve number: 2020DW-21-02). The submitted manuscript has been reviewed and authorized by the Ethics Committee.

Consent for publication

Not applicable.

Availability of data and materials

We solemnly declare that the data used in this article is real, public, and sharable. If some readers want to use original data to conduct secondary analysis, please contact corresponding author and acquire the authorization.

Competing interests

There are no conflicts of interest.

Funding

This work was supported by “Natural Science Foundation of Jiangsu Province (BK20191090)”; “Priority Academic Program Development of Jiangsu Higher Education Institutions”; “Project of Fatty Liver Research Center of Jiangsu Province Hospital of Chinese Medicine”; “The 5th Constructive Project of Inheritance Studio of Famous Old Chinese Medicine Experts in Jiangsu Province (Jiangsu Chinese Medicine Science Education [2021]7)”; and “Innovative Development Funding of Affiliated Hospital of Nanjing University of Chinese Medicine (Y2021CX31)”.

Authors' contributions

YZ and XZ contributed to conception and design of the study. XY and HW established the database and wrote the first draft of the manuscript. LZ, NW and MB were responsible for the specific procedure of experiments. JY controlled quality of the project. SL and XW performed the statistical analysis. YZ applied for research funds and modified the draft. All authors contributed to the manuscript and approved the submitted version.

Acknowledgements

Not applicable.

References

1. Ting DS, Cheung GC, Wong TY. Diabetic retinopathy: global prevalence, major risk factors, screening practices and public health challenges: a review. Clin Exp Ophthalmol 2016;44(4):260-77; doi: 10.1111/ceo.12696
2. Yau JW, Rogers SL, Kawasaki R, et al. Global prevalence and major risk factors of diabetic retinopathy. Diabetes Care 2012;35(3):556-64; doi: 10.2337/dc11-1909
3. Tan GS, Gan A, Sabanayagam C, et al. Ethnic Differences in the Prevalence and Risk Factors of Diabetic Retinopathy: The Singapore Epidemiology of Eye Diseases Study. Ophthalmology 2018;125(4):529-536; doi: 10.1016/j.ophtha.2017.10.026
4. Flaxel CJ, Adelman RA, Bailey ST, et al. Diabetic Retinopathy Preferred Practice Pattern®. Ophthalmology 2020;127(1):P66-P145; doi: 10.1016/j.ophtha.2019.09.025
5. Semeraro F, Morescalchi F, Cancarini A, et al. Diabetic retinopathy, a vascular and inflammatory disease: Therapeutic implications. Diabetes Metab 2019;45(6):517-527; doi: 10.1016/j.diabet.2019.04.002
6. Pang B, Li QW, Qin YL, et al. Traditional chinese medicine for diabetic retinopathy: A systematic review and meta-analysis. Medicine 2020;99(7):e19102; doi: 10.1097/MD.0000000000019102
7. Zhao Y, Yu X, Lou Y, et al. Therapeutic Effect of Abelmoschus manihot on Type 2 Diabetic Nonproliferative Retinopathy and the Involvement of VEGF. Evid Based Complement Alternat Med 2020;2020:5204917; doi: 10.1155/2020/5204917
8. Li EH, Huang QZ, Li GC, et al. Effects of miRNA-200b on the development of diabetic retinopathy by targeting VEGFA gene. Biosci Rep 2017;37(2):BSR20160572; doi: 10.1042/BSR20160572
9. Jiang Q, Zhao F, Liu X, et al. Effect of miR-200b on retinal endothelial cell function under high glucose environment. Int J Clin Exp Pathol 2015;8(9):10482-7.
10. Pang B, Ni Q, Di S, et al. Luo Tong Formula Alleviates Diabetic Retinopathy in Rats Through Micro-200b Target. Front Pharmacol 2020;11:551766; doi: 10.3389/fphar.2020.551766
11. Liu J, Guo S, Duan JA, et al. Analysis and utilization value discussion of multiple chemical composition in different tissues of Abelmoschus manihot. Zhongguo Zhong Yao Za Zhi 2016;41(20):3782-3791; doi: 10.4268/cjcmm20162013
12. Kim YS, Jung DH, Lee IS, et al. Osteomeles schwerinae extracts inhibits the binding to receptors of advanced glycation end products and TGF-β1 expression in mesangial cells under diabetic conditions. Phytomedicine 2016;23(4):388-97; doi: 10.1016/j.phymed.2016.02.005
13. Morikawa M, Derynck R, Miyazono K. TGF-β and the TGF-β Family: Context-Dependent Roles in Cell and Tissue Physiology. Cold Spring Harb Perspect Biol 2016;8(5):a021873; doi:

10.1101/cshperspect.a021873

14. Vander Ark A, Cao J, Li X. TGF-β receptors: In and beyond TGF-β signaling. Cell Signal 2018;52:112-120; doi: 10.1016/j.cellsig.2018.09.002
15. Bonfiglio V, Platania CBM, Lazzara F, et al. TGF-β Serum Levels in Diabetic Retinopathy Patients and the Role of Anti-VEGF Therapy. Int J Mol Sci 2020;21(24):9558; doi: 10.3390/ijms21249558
16. Tzavlaki K, Moustakas A. TGF-β Signaling. Biomolecules 2020;10(3):487; doi: 10.3390/biom10030487
17. Ladak SS, Roebuck E, Powell J, et al. The Role of miR-200b-3p in Modulating TGF-β1-induced Injury in Human Bronchial Epithelial Cells. Transplantation 2019;103(11):2275-2286; doi: 10.1097/TP.0000000000002845
18. Meng XM, Chung AC, Lan HY. Role of the TGF-β/BMP-7/Smad pathways in renal diseases. Clin Sci 2013;124(4):243-54; doi: 10.1042/CS20120252
19. Yang MC, You FL, Wang Z, et al. Salvianolic acid B improves the disruption of high glucose-mediated brain microvascular endothelial cells via the ROS/HIF-1α/VEGF and miR-200b/VEGF signaling pathways. Neurosci Lett 2016;630:233-240; doi: 10.1016/j.neulet.2016.08.005
20. Saleeb R, Kim SS, Ding Q, et al. The miR-200 family as prognostic markers in clear cell renal cell carcinoma. Urol Oncol 2019;37(12):955-963; doi: 10.1016/j.urolonc.2019.08.008
21. Jiao W, Ji JF, Xu W, et al. Distinct downstream signaling and the roles of VEGF and PlGF in high glucose-mediated injuries of human retinal endothelial cells in culture. Sci Rep 2019;9(1):15339; doi: 10.1038/s41598-019-51603-0
22. Lennikov A, Mukwaya A, Fan L, et al. Synergistic interactions of PlGF and VEGF contribute to blood-retinal barrier breakdown through canonical NFκB activation. Exp Cell Res 2020;397(2):112347; doi: 10.1016/j.yexcr.2020.112347
23. Huang H. Pericyte-Endothelial Interactions in the Retinal Microvasculature. Int J Mol Sci 2020;21(19):7413; doi: 10.3390/ijms21197413
24. Long L, Li Y, Yu S, et al. Scutellarin Prevents Angiogenesis in Diabetic Retinopathy by Downregulating VEGF/ERK/FAK/Src Pathway Signaling. J Diabetes Res 2019;2019:4875421; doi: 10.1155/2019/4875421
25. Shi Y, Chen C, Xu Y, et al. LncRNA FENDRR promotes high-glucose-induced proliferation and angiogenesis of human retinal endothelial cells. Biosci Biotechnol Biochem 2019;83(5):869-875; doi: 10.1080/09168451.2019.1569499
26. Duffy A, Liew A, O'Sullivan J, et al. Distinct effects of high-glucose conditions on endothelial cells of macrovascular and microvascular origins. Endothelium 2006;13(1):9-16; doi: 10.1080/10623320600659997
27. Xue L, Xiong C, Li J, et al. miR-200-3p suppresses cell proliferation and reduces apoptosis in diabetic retinopathy via blocking the TGF-β2/Smad pathway. Biosci Rep 2020;40(11):BSR20201545; doi: 10.1042/BSR20201545

28. Homme RP, Singh M, Majumder A, et al. Remodeling of Retinal Architecture in Diabetic Retinopathy: Disruption of Ocular Physiology and Visual Functions by Inflammatory Gene Products and Pyroptosis. Front Physiol 2018;9:1268; doi: 10.3389/fphys.2018.01268
29. Zhou L, An XF, Teng SC, et al. Pretreatment with the total flavone glycosides of Flos Abelmoschus manihot and hyperoside prevents glomerular podocyte apoptosis in streptozotocin-induced diabetic nephropathy. J Med Food 2012;15(5):461-8; doi: 10.1089/jmf.2011.1921
30. Wan Y, Wang M, Zhang K, et al. Extraction and determination of bioactive flavonoids from Abelmoschus manihot (Linn.) Medicus flowers using deep eutectic solvents coupled with high-performance liquid chromatography. J Sep Sci 2019;42(11):2044-2052; doi: 10.1002/jssc.201900031
31. Qiu J, Zhang T, Zhu X, et al. Hyperoside Induces Breast Cancer Cells Apoptosis via ROS-Mediated NF-κB Signaling Pathway. Int J Mol Sci 2019;21(1):131; doi: 10.3390/ijms21010131
32. Lin YT, Lin HR, Yang CS, et al. Antioxidant and Anti-α-Glucosidase Activities of Various Solvent Extracts and Major Bioactive Components from the Fruits of *Crataegus pinnatifida*. Antioxidants (Basel) 2022;11(2):320; doi: 10.3390/antiox11020320
33. Wu W, Xie Z, Zhang Q, et al. Hyperoside Ameliorates Diabetic Retinopathy via Anti-Oxidation, Inhibiting Cell Damage and Apoptosis Induced by High Glucose. Front Pharmacol 2020;11:797; doi: 10.3389/fphar.2020.00797
34. Ku SK, Kwak S, Kwon OJ, et al. Hyperoside inhibits high-glucose-induced vascular inflammation in vitro and in vivo. Inflammation 2014;37(5):1389-400; doi: 10.1007/s10753-014-9863-8
35. Sohn E, Kim J, Kim CS, et al. Osteomeles schwerinae Extract Prevents Diabetes-Induced Renal Injury in Spontaneously Diabetic Torii Rats. Evid Based Complement Alternat Med 2018;2018:6824215; doi: 10.1155/2018/6824215
36. Mrugacz M, Bryl A, Zorena K. Retinal Vascular Endothelial Cell Dysfunction and Neuroretinal Degeneration in Diabetic Patients. J Clin Med 2021;10(3):458; doi: 10.3390/jcm10030458
37. Zhang D, Lv FL, Wang GH. Effects of HIF-1α on diabetic retinopathy angiogenesis and VEGF expression. Eur Rev Med Pharmacol Sci 2018;22(16):5071-5076; doi: 10.26355/eurrev_201808_15699
38. Wang N, Zhu F, Shen M, et al. Network pharmacology-based analysis on bioactive anti-diabetic compounds in Potentilla discolor bunge. J Ethnopharmacol 2019;241:111905; doi: 10.1016/j.jep.2019.111905
39. Bai L, Li X, He L, et al. Antidiabetic Potential of Flavonoids from Traditional Chinese Medicine: A Review. Am J Chin Med 2019;47(5):933-957; doi: 10.1142/S0192415X19500496
40. Vasishta S, Umakanth S, Adiga P, et al. Extrinsic and intrinsic factors influencing metabolic memory in type 2 diabetes. Vascul Pharmacol 2022;142:106933; doi: 10.1016/j.vph.2021.106933
41. Chen Z, Natarajan R. Epigenetic modifications in metabolic memory: What are the memories, and can we erase them? Am J Physiol Cell Physiol 2022;323(2):C570-C582; doi: 10.1152/ajpcell.00201.2022

42. Ogura S, Kurata K, Hattori Y, et al. Sustained inflammation after pericyte depletion induces irreversible blood-retina barrier breakdown. JCI Insight 2017;2(3):e90905; doi: 10.1172/jci.insight.90905

Figures

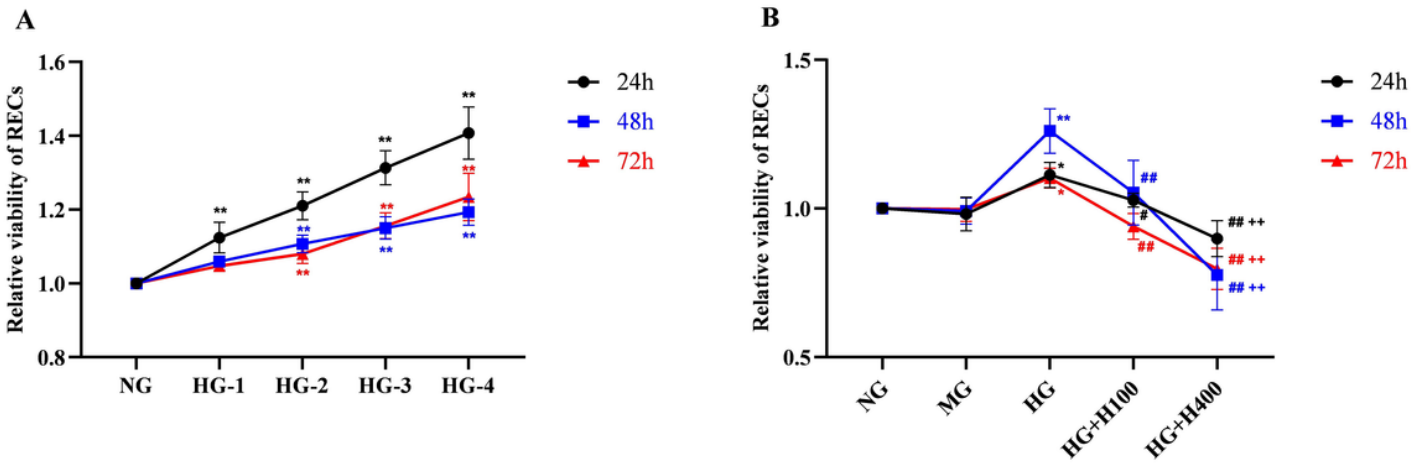

Figure 1

RECs viability was positively correlated with glucose concentration and obviously inhibited by hyperoside. (**A**) The relative viability of RECs in different concentrations of glucose was measured by CCK-8 after 24h, 48h, and 72h of incubation. (**B**) The relative viability of RECs in NG, MG, HG, HG+HY100 and HG+HY400 were measured by CCK-8 after 24h, 48h, and 72h of incubation. RECs in HG+H100 and HG+H400 were transferred to high-glucose mediums and were added with 100 ug/mL and 400 ug/mL hyperoside for further incubation, respectively. Data are presented as mean ± standard deviation. $P<0.05$ is statistically significant. * vs. NG, $P<0.05$, ** vs. NG, $P<0.01$, $^{\#}$ vs. HG, $P<0.05$, $^{\#\#}$ vs. HG, $P<0.01$, $^{++}$ vs. HG+H100, $P<0.01$.

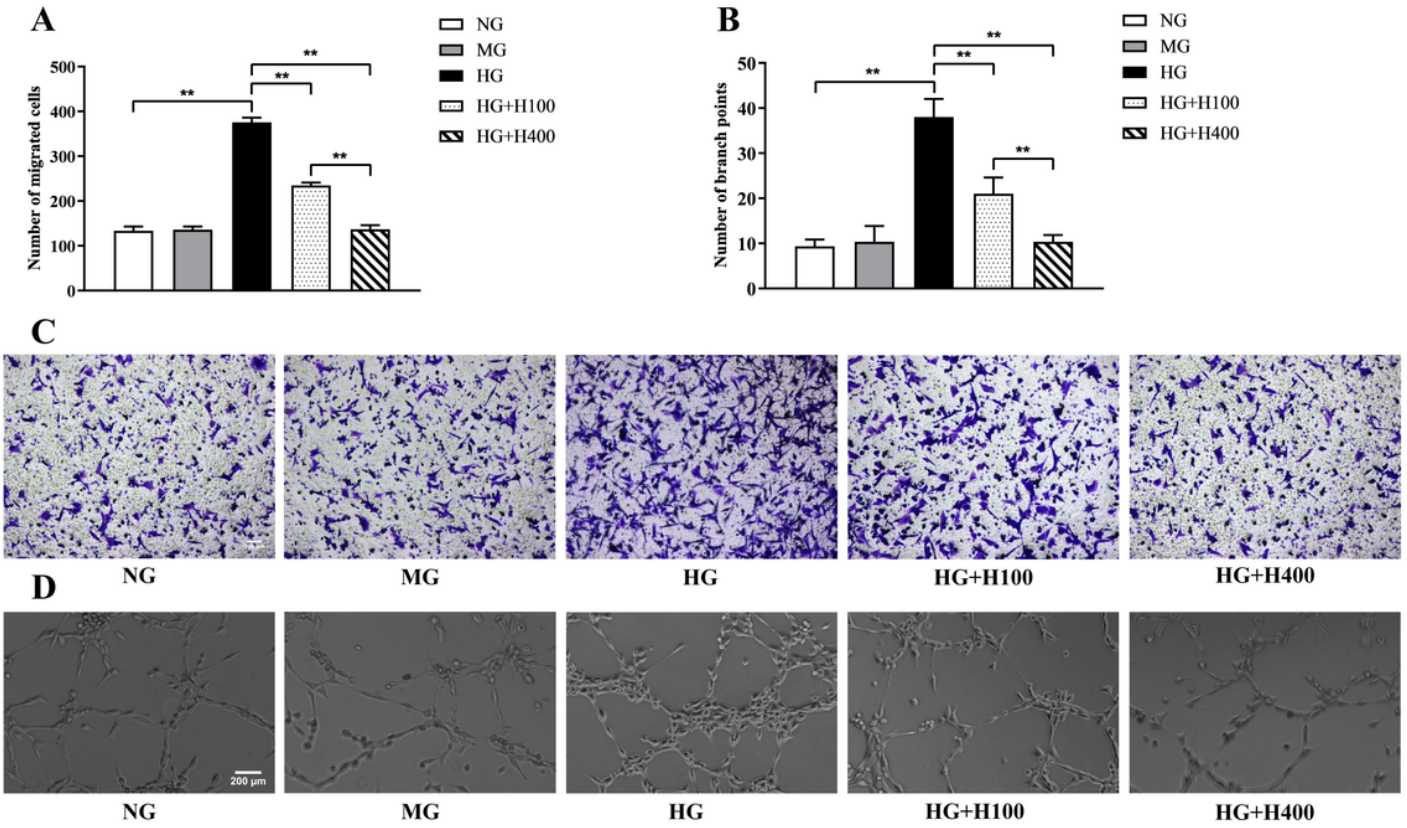

Figure 2

The excessive migration and tube formation of RECs were induced by high glucose and inhibited by hyperoside. (**A**) The comparison of migrated RECs measured by transwell assay in HG and different concentrations of hyperoside. (**B**) The comparison of RECs branch points tested by tube formation assay in HG and different concentrations of hyperoside. (**C**) The representative pictures of transwell assay in different groups under the microscope (× 200). (**D**) The representative pictures of tube formation assay in different groups under the microscope (× 200). Data are presented as mean ± standard deviation. $P<0.05$ is statistically significant. ** $P<0.01$.

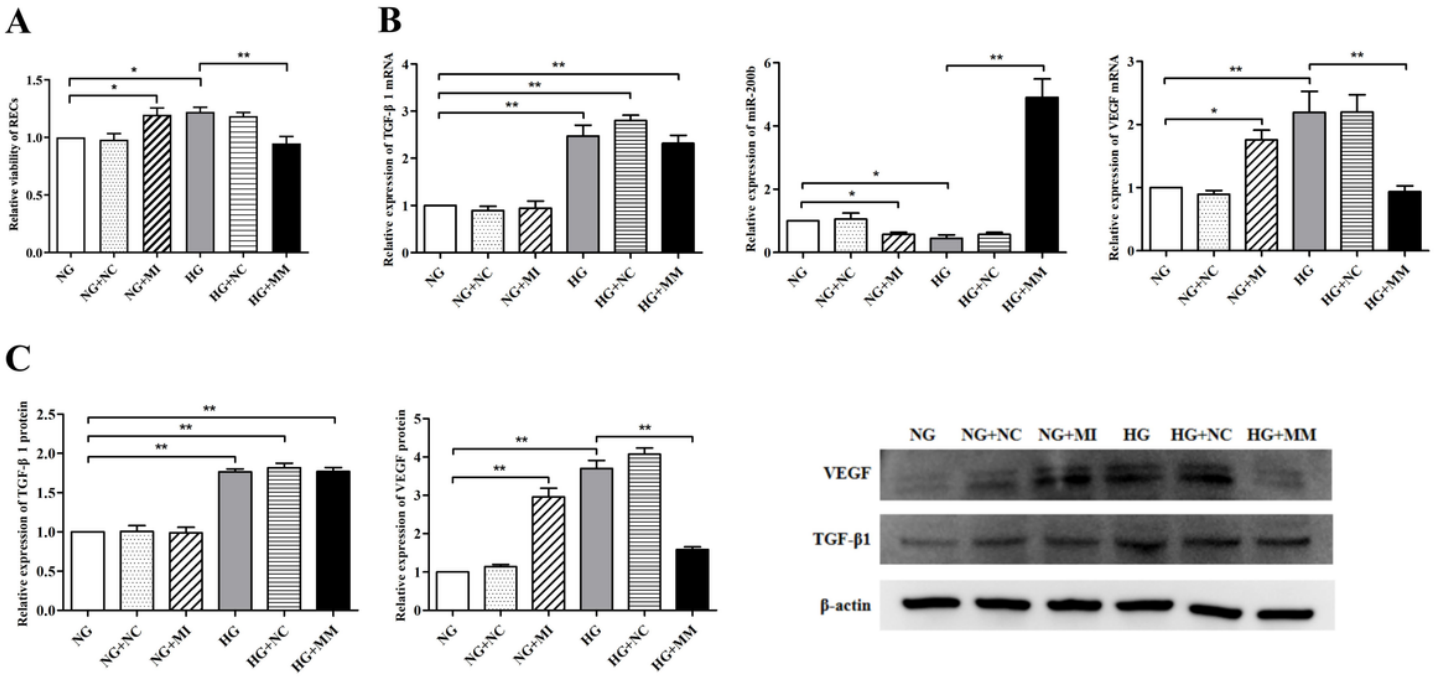

Figure 3

TGF-β1/miR-200b/VEGF pathway played a key role in high-glucose-induced proliferation of RECs. **(A)** The viability of RECs in all groups was measured by CCK-8 after transfection. **(B)** The expressions of TGF-β1 and VEGF mRNAs and miR-200b in different groups were assayed by qRT-PCR after transfection. **(C)** The expressions of TGF-β1 and VEGF proteins in different groups were detected by WB after transfection. Data are presented as mean ± standard deviation. $P<0.05$ is statistically significant. * $P<0.05$, ** $P<0.01$.

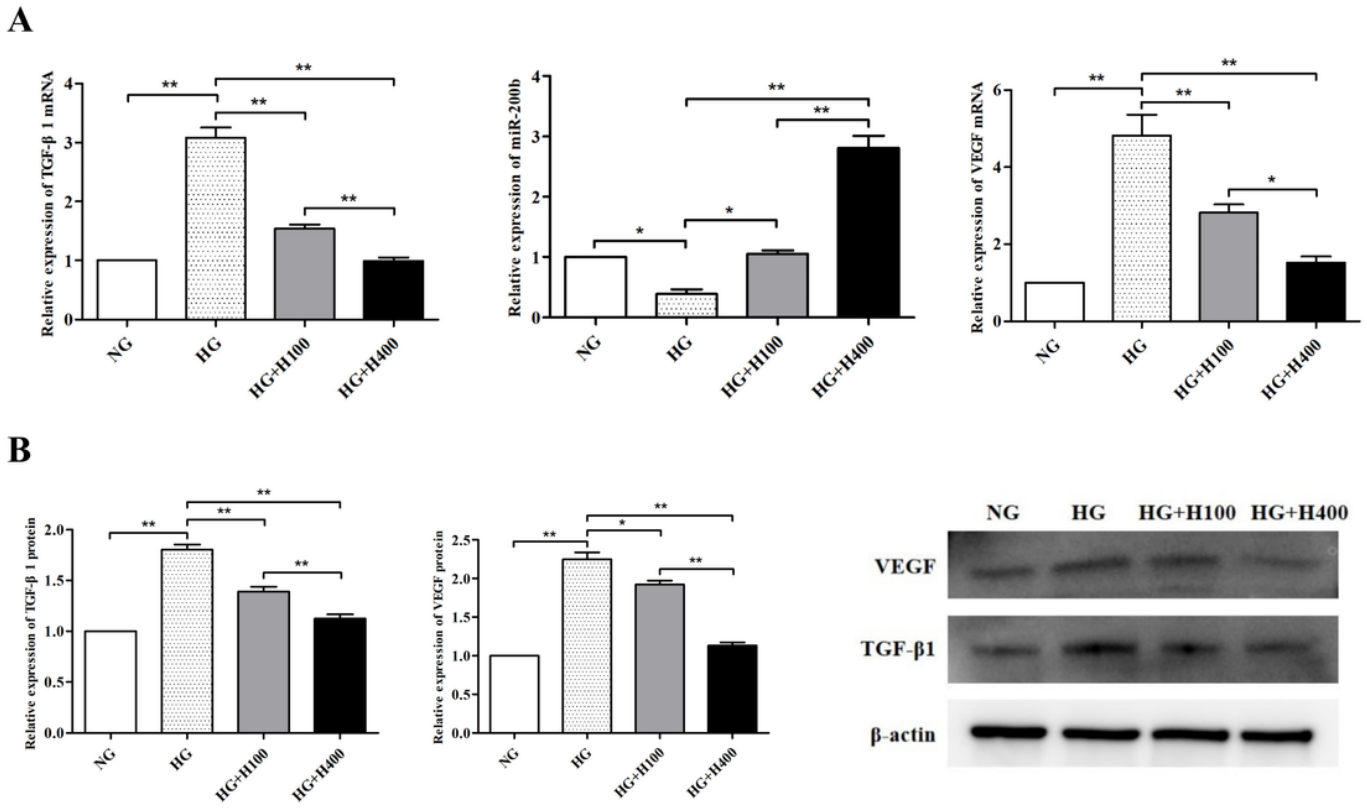

Figure 4

Hyperoside downregulated TGF-β1 & VEGF and upregulated miR-200b of RECs in high glucose. **(A)** The expressions of TGF-β1 and VEGF mRNAs and miR-200b in different groups were tested by qRT-PCR. **(B)** The expressions of TGF-β1 and VEGF proteins in different groups were detected by WB. Data are presented as mean ± standard deviation. P<0.05 is statistically significant. * P<0.05, ** P<0.01.

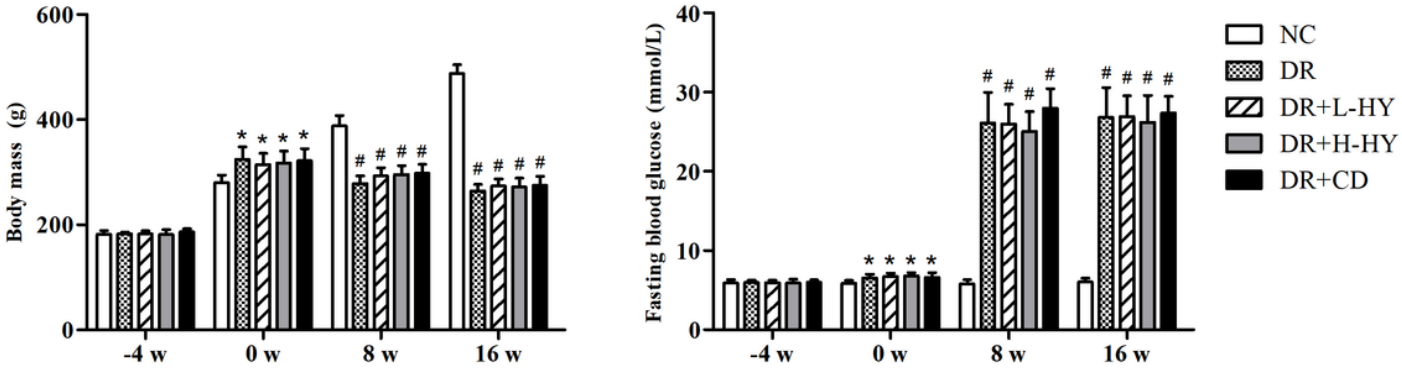

Figure 5

The comparisons of BM and FBG of rats were performed at different times. The BM and FBG of rats are all measured on fasting in the morning. Data are presented as mean ± standard deviation. P<0.05 is

statistically significant. * vs. NC at the same week, P<0.05; # vs. NC at the same week, P<0.01.

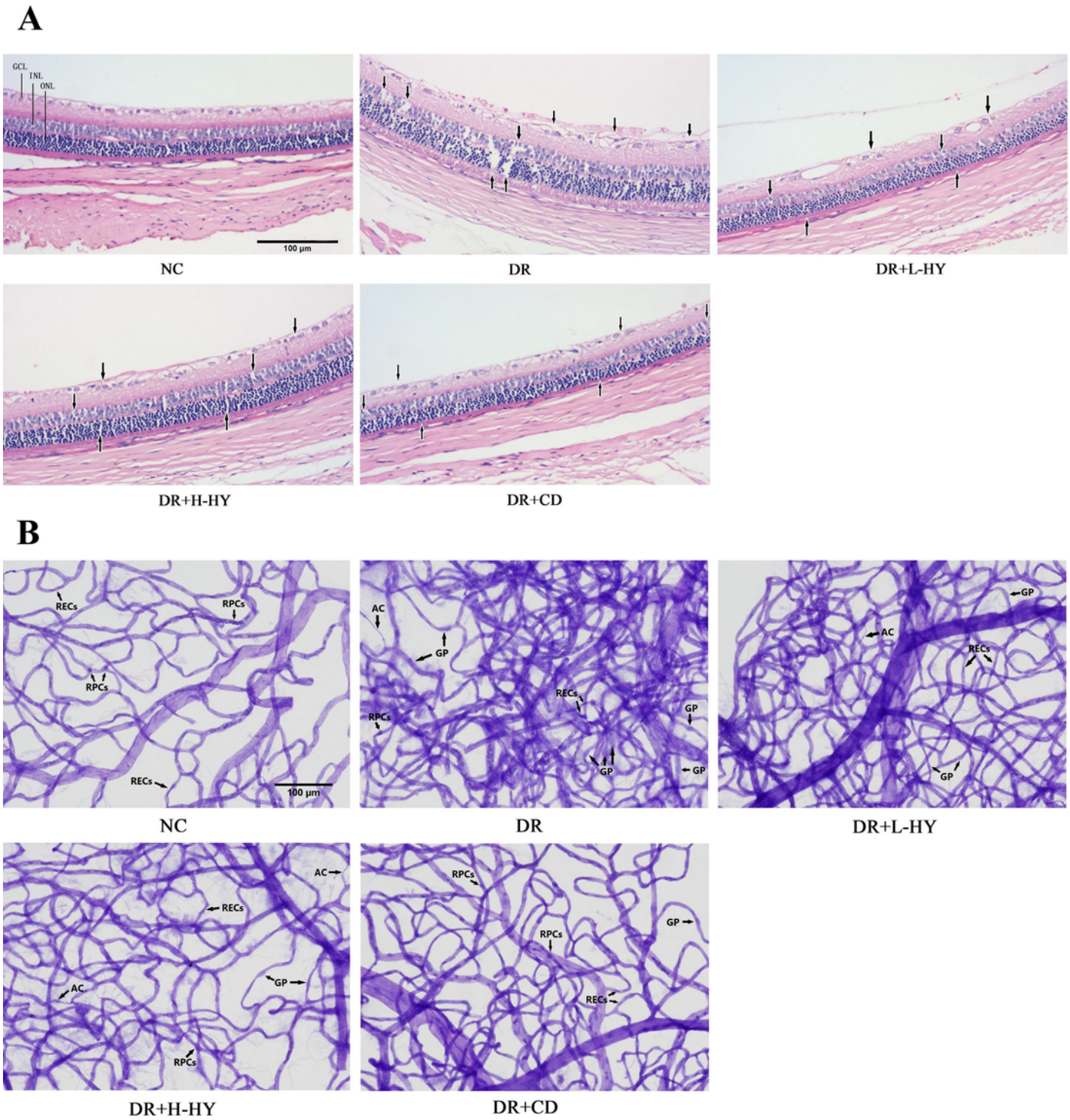

Figure 6

The representative pathological changes of retinal tissues and the typical images of retinal vasculopathy in different groups. **(A)** The pathological changes of retinal tissue were detected by HE staining. (HE × 200). **(B)** The retinal vasculopathy was detected by retinal trypsin digest and PAS staining. (PAS × 200). GCL: ganglion cell layer; INL: inner nuclear layer; ONL: outer nuclear layer; RECs: retinal endothelial cells; RPCs: retinal pericytes; AC: acellular capillaries; GP: ghost-pericytes. The differences of pathological changes and retinal vasculopathy in all groups were indicated by black arrows.

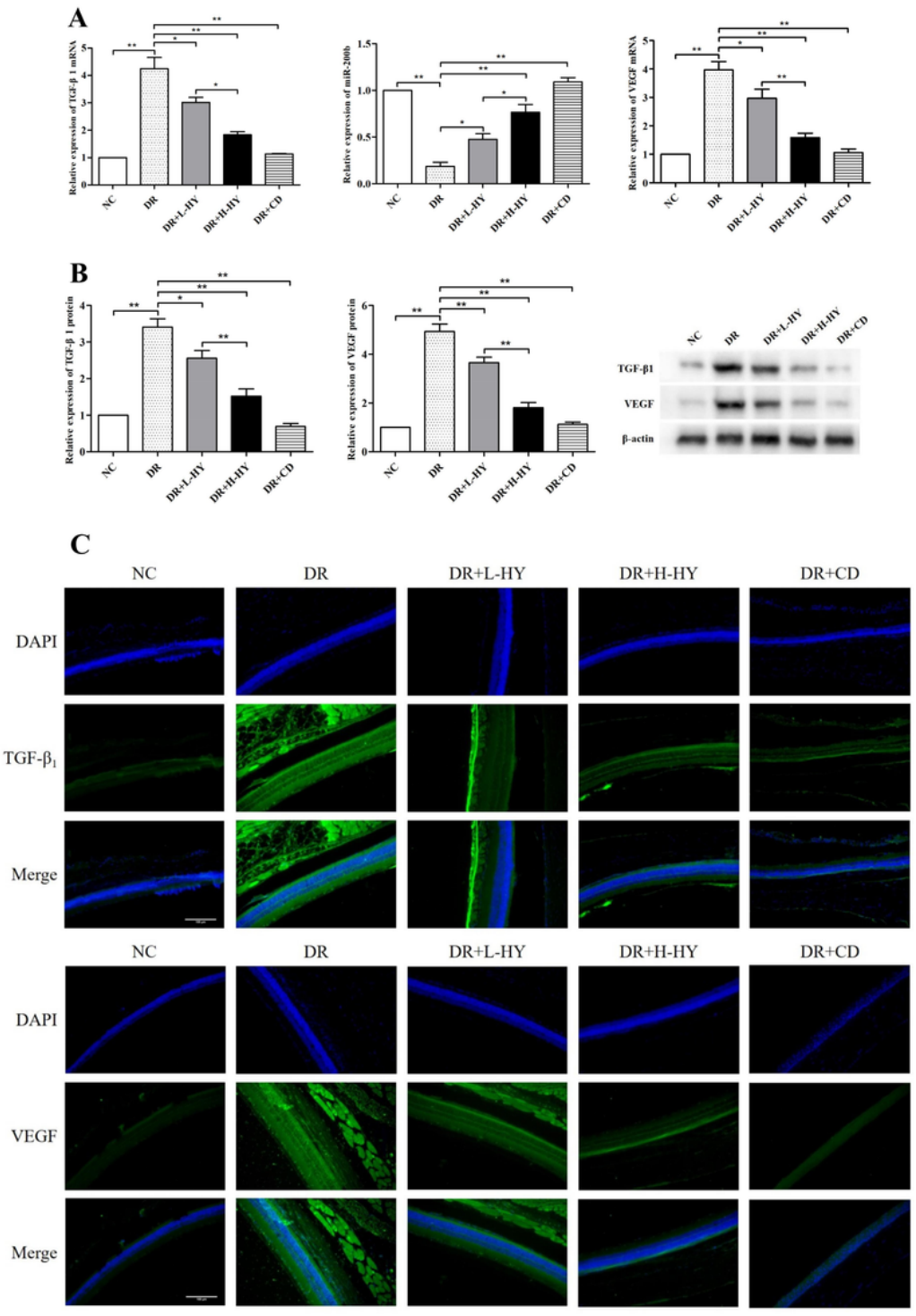

Figure 7

Hyperoside downregulated TGF-β1 & VEGF and upregulated miR-200b in retinal tissues of DR rats. **(A)** The expressions of TGF-β1 and VEGF mRNAs and miR-200b in different groups were tested by qRT-PCR. **(B)** The expressions of TGF-β1 and VEGF proteins in different groups were detected by WB. **(C)** The representative images of TGF-β1 and VEGF proteins were detected by IF in different groups. (IF × 200). Green fluorescence represented FITC-labeled TGF-β1 and VEGF levels in retinal tissues, and blue fluorescence represented DAPI-stained retinal cells. Data are presented as mean ± standard deviation. $P<0.05$ is statistically significant. * $P<0.05$, ** $P<0.01$.

Supplementary Files

This is a list of supplementary files associated with this preprint. Click to download.

- Figure3TGF1.tif
- Figure3VEGF.tif
- Figure3actin.tif
- Figure4TGF1.tif
- Figure4VEGF.tif
- Figure4actin.tif
- Figure7TGF1.tif
- Figure7VEGF.tif
- Figure7actin.tif